

# AmphiHex-I: Locomotory Performance in Amphibious Environments With Specially Designed Transformable Flipper Legs

Shiwu Zhang, *Member, IEEE*, Youcheng Zhou, Min Xu, Xu Liang, Jiming Liu, *Fellow, IEEE*, and Jie Yang

**Abstract**—An amphibious robot can locomote in amphibious environments, including walking on rough terrains, maneuvering underwater, and passing through soft muddy or sandy substrates in the littoral area between land and water. However, developing an amphibious robot is challenging, especially when it requires a high locomotory performance in soft substrates and a combination of different propulsion methods. To tackle such a challenge, an amphibious robot, known as AmphiHex-I, with novel transformable flipper-leg composite propulsion mechanisms has been proposed and developed. In this paper, locomotory performance of the flipper legs in amphibious environments, especially in the muddy terrain, is extensively studied with a walking platform in terms of structural parameters, kinematic parameters, and environmental properties. The results indicate that there exist an optimal rotation speed of the flipper legs with various shapes for a higher locomotion speed of the walking model in muddy terrain, which guides the design and the control of the transformable flipper legs. Through the versatile gaits of AmphiHex-I in amphibious environments, outdoor locomotion experiments validate the platform study and demonstrate that the robot's transformable flipper-leg propulsion mechanisms make it highly adaptive to a littoral environment such as the muddy terrain. Locomotion ability of AmphiHex-I endows its broad applications in the areas of resource exploration, disaster rescue, and reconnaissance in complex environments.

**Index Terms**—Amphibious environments, amphibious robot, gait, locomotory performance, transformable flipper leg.

## I. INTRODUCTION

ROBOTS that are able to swim underwater or pass through rough terrains have been developed and applied

Manuscript received March 13, 2015; revised August 23, 2015; accepted October 1, 2015. Date of publication October 12, 2015; date of current version April 28, 2016. Recommended by Technical Editor Y.-J. Pan. This work was supported by the National Natural Science Foundation of China (51375468, 50975270).

S. Zhang, Y. Zhou, M. Xu, X. Liang, and J. Yang are with the Department of Precision Machinery and Precision Instrumentation, University of Science and Technology of China, Hefei 230026, China (e-mail: swzhang@ustc.edu.cn; zhouyoucheng1987@126.com; xumin@ustc.edu.cn; jay08009@mail.ustc.edu.cn; jieyang@ustc.edu.cn).

J. Liu is with the Department of Computer Science, Hong Kong Baptist University, Kowloon, Hong Kong (e-mail: Jiming@comp.hkbu.edu.hk).

This paper has supplementary downloadable material available at <http://ieeexplore.ieee.org> provided by the authors. This includes a video showing the locomotion ability of AmphiHex-I. This material is 14 MB. Contact swzhang@ustc.edu.cn for further questions about this work.

Color versions of one or more of the figures in this paper are available online at <http://ieeexplore.ieee.org>.

Digital Object Identifier 10.1109/TMECH.2015.2490074

successfully in many fields. However, amphibious robots, which simultaneously adapt to various complex environmental conditions, such as rough terrains, littoral areas, and water, have not been as successful despite being in acute demand for exploration and rescue under these conditions. Amphibious robots incorporate propulsion mechanisms used on land and underwater into one body. However, the land and underwater mechanisms are quite different [1]. Underwater propulsion mechanisms push against fluids and create vortices that represent the mechanisms' exertion of momentum, and propulsion mechanisms on land usually push against hard surfaces on rough terrains, producing an opposite reaction force or a friction force to propel the robots. The difference in propulsion is also reflected in the fin/limb transition resulting from the evolution of fish into tetrapods [2]. An amphibious robot usually uses two propulsion mechanisms to conquer various environments, which necessitates a bulky structure and compromises locomotory performance. In addition to the issue of composite propulsion mechanisms, a complex amphibious environment presents many difficulties in relation to the locomotion of amphibious robots. The amphibious environment includes not only various rough terrains such as rocks, grass, and gravel, but also various watery environments such as rivers, lakes, and seas. Beyond land and water, one of the most important environments an amphibious robot must conquer is often ignored. There often exists a large littoral area between water and rough terrains. This littoral area is often full of soft substrates, such as wet sand and mud. The physical properties of substrate materials significantly affect a robot's locomotory performance [3], [4]. Muddy or sandy substrates are easily transformed or destroyed when a propulsion mechanism pushes against them. The "soft" properties of the substrates lead to a loss of locomotory performance, which is a great challenge for amphibious robots to address. Sandy substrates can be considered as a granular media with rheological characteristics, and behave like an elastic solid below the limited stress and a fluid above the limited stress. Locomotion in dry sand has been examined to develop bioinspired robots in desert environments and to reveal the locomotion of desert-living organisms [5]–[7]. However, locomotion in muddy substrates has not been well explored despite its importance to amphibious robots.

Some promising amphibious robots have been developed and demonstrated in recent years. In general, the current amphibious robots can be classified into two categories. The first category of robots uses two sets of propulsion mechanisms and switches between them to adapt to water and rough terrains [8]–[10]. The typical robots of the category include AmphiRobot-1 that integrates wheeled propulsion and fish-like swimming [9], [11], and the amphibious Salamander robot that uses body undulation

and limb rotation to propel [10], [12], [13]. However, the design of these two sets of propulsion mechanisms increases the structural complexity and decreases the payload of the robots. The second category of robots uses one set of mechanisms for both underwater and terrain propulsion [14]–[18]. The typical robots include Whegs that combines a propeller with a wheel leg [19], [20], and ACM-R5 that undulates its body to propel [21]. Sharing the same propulsion mechanism increases the robot's payload. However, the physical properties of various environments present different requirements. Unchanged propulsion mechanisms may lead to difficulties during the transition between water and terrains.

In summary, the dynamics of locomotion in amphibious environments is very complicated, as locomotory performance involves not only the structural characteristics of propulsion mechanisms, but also the physical properties of the environments. An effective composite propulsion mechanism that can conquer rough terrains, underwater environments, and especially soft littoral areas is critically essential for an amphibious robot. To address this problem, an amphibious robot, known as AmphiHex-I, with composite propulsion mechanisms that can transform from straight flippers to curved legs has been developed [22], [23]. Preliminary experimental results demonstrate the adaptiveness of the robot in various environments. However, as mentioned before, the locomotory performance of the robot in littoral areas and the transition between various environments are vital for the amphibious robot and need to be addressed. In this paper, we focus on the locomotory performance of AmphiHex-I in soft muddy terrain in relation to the special design of the transformable flipper legs and the gaits adopted. Two-legged free walking platform has been developed to study the locomotory performance in terms of flipper legs' structural parameters, kinematic parameters, and environmental properties, which guides the design and the control of the transformable flipper leg. The extensive experiments on field locomotion of the robot with various gaits have demonstrated and verified the effectiveness of the especially designed transformable flipper legs' locomotion in muddy terrain. Robot's locomotion on rough terrains and underwater also implies the adaptability of the robot in amphibious environments, which endows AmphiHex-I broad applications in the areas of resource exploration, disaster rescue, and reconnaissance in complex environments.

The remainder of this paper is organized as follows. Section II describes the mechanical design of the transformable flipper leg based on the locomotory performance of curved legs in muddy terrain and transformation force analysis. Section III describes AmphiHex-I's versatile gaits and gait. The experimental results are summarized in Section IV. Finally, Section V discusses future work and concludes this paper.

## II. SPECIAL DESIGN OF TRANSFORMABLE FLIPPER LEG

Various environments present different requirements for propulsion mechanisms. An amphibious robot can propel itself underwater, on rough terrains, and in littoral areas by transforming its propulsion mechanisms. In view of the aforementioned issues, the objective of developing a transformable propulsion

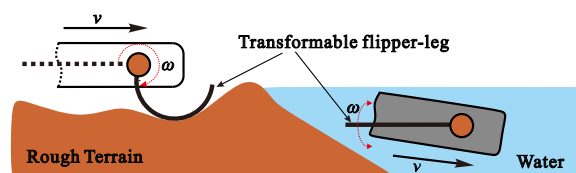


Fig. 1. Amphibious robot occupied by a transformable flipper-leg propulsion mechanism.

mechanism includes exploring the effective propulsion mechanisms in the soft substrates of littoral areas and selecting proper propulsion mechanisms with similar structures that can easily transform into one another.

### A. Transformable Flipper Leg of AmphiHex-I

Wheeled locomotion is widely used on land, as it has a high locomotion speed and is highly efficient on hard flat terrain. Legged locomotion is another popular propulsion method suitable for rough terrains [24]. Curved legs that incorporate the advantages of legged and wheeled locomotion have recently achieved great success on rough terrains. One typical robot that adopts curved legs as propulsion mechanisms is the RHex series robot [25], [26]. Although a curved leg has the advantage on rough terrains, it does not work well underwater. Inspired by the ways in which fish undulating their bodies or oscillate their appendages to swim underwater, many biomimetic underwater vehicles have also been developed [27]–[31]. Underwater undulation/oscillation propulsion is highly efficient and maneuverable. The use of multiple appendages oscillating to propel a robot underwater is an optimal way to guarantee an effective payload. The AQUA series robot uses six flippers oscillating as propulsion mechanisms underwater and can achieve plenty of aquatic maneuvers [8].

In summary, curved legs have been verified as effective for locomotion on rough terrains, and straight flippers are a good option for underwater propulsion due to their simple structure and high propulsion performance. Thus, a straightforward solution is to transform a straight flipper into a curved leg when the robot encounters an environmental transition. As shown in Fig. 1, amphibious robots such as those in the RHex series can rotate a curved leg to locomote on rough terrains. When the robot enters water, the curved leg can transform into a straight flipper, and the robot can swing the leg to propel itself underwater in the way turtles or AQUA robots do. Transforming a straight flipper into a curved leg is relatively simple and easy to accomplish. AmphiHex-I, which incorporates six transformable flipper legs into one body and can overcome the limitations of the current propulsion mechanisms, has been proposed and developed [22], [23]. The initial study demonstrates that AmphiHex-I can achieve various maneuvers underwater with six flippers acting as vectored thrusters. Furthermore, with its six curved legs composing various gaits, AmphiHex-I is suitable for terrestrial locomotion as RHex series robot do.

The design concept of the transformable flipper leg of AmphiHex-I is presented in Fig. 2. For the sake of simplicity, reliability, and easy control, the flexible cable driven by a motor with a self-locking mechanism was adopted to transform the flipper leg. The body of the transformable flipper leg is

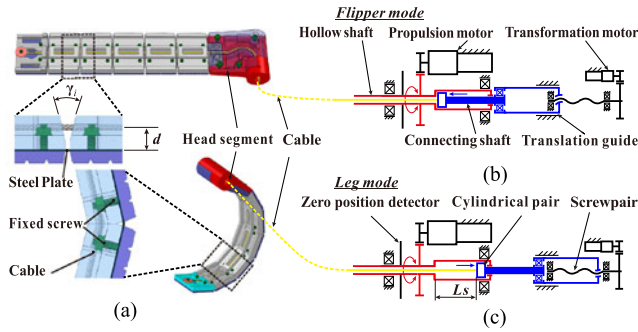


**Fig. 2.** Mechanical design of the amphibious transformable flipper leg. (a) Structure of the flipper leg,  $d$  denotes the distance from the cable to the steel plate; (b) and (c) driving module of the flipper leg,  $L_s$  denotes the translational distance of the cable that pulls the leg from straight to circled status.

composed of several types of segments. All of the segments are connected by a thin piece of elastic steel plate, which endows the flipper leg with a certain flexibility when it is not in its final curved state. A flexible cable runs continuously through all of the segments and is fixed to the end segment. Angle  $\gamma_i$  in Fig. 2(a) is formed by two inclined planes that belong to two adjacent segments, and determines the final shape of the curved leg when the cable is pulled tightly. However, when the cable is loosened, the flipper leg transforms into a straight flipper due to the elastic force generated by the steel plate. The key problem for a flipper-leg driving module is to achieve transformation motion and propulsion motion without a collision. Here, we adopt a cylindrical joint and a screw pair to achieve such a coupled motion, as shown in Fig. 2(b) and (c). The flexible cable is connected to the connecting shaft through a hollow shaft. The connecting shaft can slide in the groove of the hollow shaft during transformation, and can rotate along with the rotation of the hollow shaft driven by a propulsion motor. The connecting shaft is connected to the nut of a screw pair which can perform a translational motion driven by a transformation motor to realize the translational movement of the cable.

The overall design of the structure and the control system of AmphiHex-1 can refer to [22] and [23]. The locomotory performance of the robot mainly depends on the structure of the flipper legs and the gaits adopted accordingly. For the design of the transformable flipper leg, the key parameters include the thickness of the steel plate  $d_s$ , which determines the transformation force of the flipper leg and the propulsion force during swimming, and the angles  $\gamma_i$ , which determine the final shape of the flipper leg when it is in curved leg mode, and further affect the locomotory performance on various terrains.

### B. Curved Legs in Muddy Terrain

Littoral environment often includes soft terrains such as sandy terrain or muddy terrain. Unlike locomotion in sandy terrain, locomotion in muddy terrain still remains unexplored for the unrevealed non-Newton characteristics of the muddy substrate. Fig. 3(a) presents the situation that AmphiHex-I entering water from muddy bank. The supportive legs of AmphiHex-I were totally immersed in the muddy substrate, which brings a difficulty for the locomotion of the robot. Exploring and enhancing

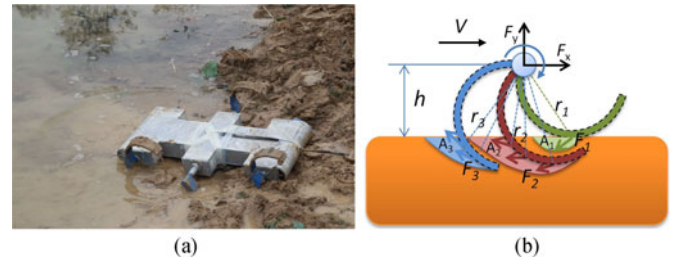


**Fig. 3.** Curved legs in muddy terrain. (a) AmphiHex-I entering water from muddy bank. (b) Analysis of curved legs in muddy terrain.

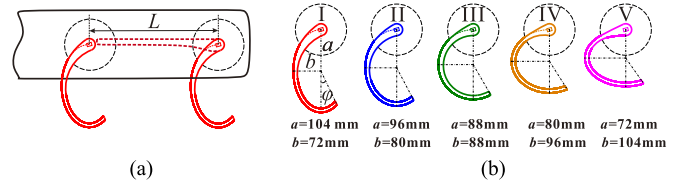


**Fig. 4.** Shape of curved legs. (a) Structural constraint for the length of transformable flipper leg. (b) Five types of curved legs with the same length.

locomotory performance in soft muddy terrain are vital for the applications of AmphiHex-I.

Locomotion with rotating curved legs in muddy terrain can be analyzed in Fig. 3(b). When a curve-legged robot passes through muddy substrate, the radius from the rotation center to the contact part of the leg varies ( $r_i$ ), which means that the soft materials that are pushed away (or destroyed) by the curved leg during locomotion [ $A_i$  in Fig. 3(b)] vary along with the leg rotating. The pushed materials provide a reaction force to support and propel the robot, which benefits the locomotory performance. According to the analysis, the shape of the curved leg will also affect the volume of the destroyed materials and further vary the magnitude of the supportive and propulsion forces. That is, the shape of the curved leg affects the locomotory performance in muddy terrain, which should be studied in the special design of the flipper leg.

A series of curved legs was designed for AmphiHex-I to explore the influence of the shape of the curved legs on locomotory performance in muddy terrain. The length of the legs in their straight flipper state stays constant, which is more reasonable than the design of legs with the same height in the initial study [23]. As shown in Fig. 4(a), the length of the flipper leg in its straight state  $L$  cannot be larger than the distance between the rotation axes of the two neighboring flipper legs to avoid interference during underwater oscillation. Moreover, decreasing the length of the flipper legs may lead to a lower locomotory performance underwater and on rough terrains. Fig. 4(b) shows five types of curved legs with a fixed length  $L$ . According to the figure, changing the length of the semielliptical major axis ( $a$  and  $b$ ) introduces a series of leg shapes. The shape of Leg III is set as a semicircle with a radius of 88 mm.  $\phi$  is set at  $30^\circ$ , which extends the angle of the sector and decreases the fluctuation of the robot. From Legs I to V, the shape of the legs changes from a straight state to a bent state.

Locomotion in muddy terrain is complicated, and involves a complex interaction between the propulsion mechanism and muddy substrate that is often considered a type of non-Newton

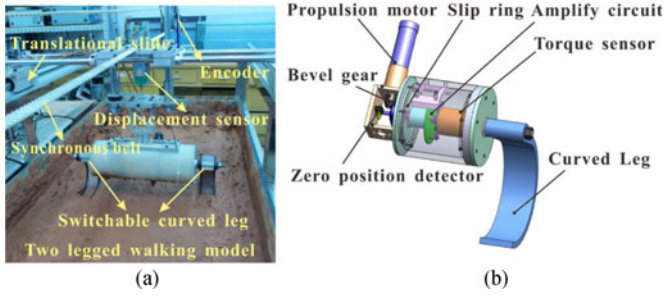


Fig. 5. Two-legged free walking platform for the leg-terrain interaction. (a) Overview of the platform; (b) design of single leg unit.

fluid. The constitutive force equation of a muddy substrate with various water content levels is also complicated, and there remains a lack of intensive study of the effect on such a non-Newton fluid. Studies have estimated the influence of leg shape on locomotory performance on sandy substrate using the RFT model or its revised model [22], [23], [32], [33]. However, the RFT model does not work well when applied to locomotion in muddy substrate [33]. Fortunately, the locomotory performance in muddy terrain can be estimated experimentally. The influence of leg shape, the kinematic parameters, and the properties of muddy substrate on locomotory performance are explored in the next section, which is very important for the selection of leg structure and a control strategy.

### C. Two-Legged Free Walking Experiment

We developed a two-legged free walking experimental platform equipped with various sensors to explore the locomotory performance of different curved legs in muddy substrate. The platform was similar to the wheel-terrain test bed [34]. We used it to obtain data related to the robot's motor torque output, height variation, and locomotion speed during walking. Fig. 5 illustrates the setup of the two-legged platform. The tank was  $1850 \times 800 \times 500$  mm in length  $\times$  width  $\times$  depth, which was large enough to accommodate muddy substrate with a certain water content to eliminate the boundary effect. A two-legged free walking model was installed on the two translational slides. One horizontal slide was dragged by a synchronous belt rotating with a rotary encoder (resolution: 1000 P/R), which was used to measure the forward speed of the two-legged walking model. The other slide was perpendicular and attached to a displacement sensor (range: 175 mm with a linear accuracy of 0.05%), and was used to monitor the variation of the height of the model during walking. Furthermore, two torque sensors (range: 10 N·m with an accuracy of 0.5% F.S) that connected the output shaft of the motors and the curved legs were used to measure the torques that drove the curved legs during walking.

We gathered the mud used in the experiment from the bank of a river and filtered it to keep it homogeneous. We defined the mud's water content as the ratio of the mass of the water contained in the mud to the total mass of the mud. We adopted four water content levels in the experiment, including 23%, 25%, 27%, and 29%. Mud with a 23% water content was relatively hard, and mud with a 29% water content was akin to a fluid. We stirred the mud in the tank before each free walking to ensure that the water content was uniform. We adopted six angular ve-

locities for the legs in the experiments, including 1, 2, 3, 4, 5, and 6 rad/s, respectively. To explore the influence of the characteristics of the curved legs (leg shapes), kinematic parameters (angular velocities of the legs), and littoral environment (water content) on locomotory performance, we adopted synchronous gaits for the two legs with various angular velocities. The synchronous gait increased the fluctuation of the gravity center, and the performance of the locomotion model was similar to that of the single-leg model. The synchronous gait adopted in the experiments was also different from the gait adopted in the initial study [23], where the walking model adopted an asynchronous gait. The asynchronous gait incorporates more gait factors in the locomotion, and hinders extracting the influence of the structural, kinematic, and substrate characteristics on the locomotory performance.

In the experiments, we selected three parameters to evaluate the locomotory performance of the two-legged free walking model, including the average forward speed, propulsion efficiency, and height variant of the center of gravity (CG). The average forward speed and the height variant of CG can be measured from the sensors, respectively. The propulsion efficiency  $\eta$  is defined as the multiplicative inverse of the cost of transport, which is borrowed from the evaluation of animal locomotion [35]. Here, propulsion efficiency is defined as forward moving distance of the model divided by the energy it costs. It can be formulated as

$$\eta = \frac{\Delta l}{W} \quad (1)$$

where  $\Delta l$  denotes the displacement of the walking model when the legs rotate one cycle.  $W$  denotes the energy consumed during the period, and can be calculated by

$$W = \int_0^{2\pi} (T_l \omega_l + T_r \omega_r) d\theta \quad (2)$$

where  $T_l$  and  $T_r$  stand for the torque outputs of the motors for the left and right curved legs, respectively.  $\omega_l$  and  $\omega_r$  represent the angular velocity of the left and right curved legs, respectively.  $\theta$  denotes the angular displacement of the curved legs.

### D. Littoral Walking Results Analysis

Based on the preceding experimental platform and definitions, we conducted extensive experimental study on the locomotory performance of the curved legs in muddy substrate. Fig. 6(a)–(d) displays the forward speed of the two-legged walking model in relation to the angular velocity of the legs, the water content of the mud, and the leg shapes. The figure reveals two facts. First, the forward speed decreased from the straight legs to bent legs (Legs I–V) for all of the water content levels. However, the advantage was not so obvious where the water contents were 23% and 29%. The forward speed was higher when the water content was lower for the same shape and angular velocity. Second, in the case of the lower water content level (23%), the forward speed had an approximate linear relationship with the angular velocity of the legs, which persisted in the case of the higher water content level (29%). However, when the water content level was medial (25% and 27%), the dynamics of the forward speed could be classified into three categories. The first was the forward speed of Legs I, II, III in 25% water

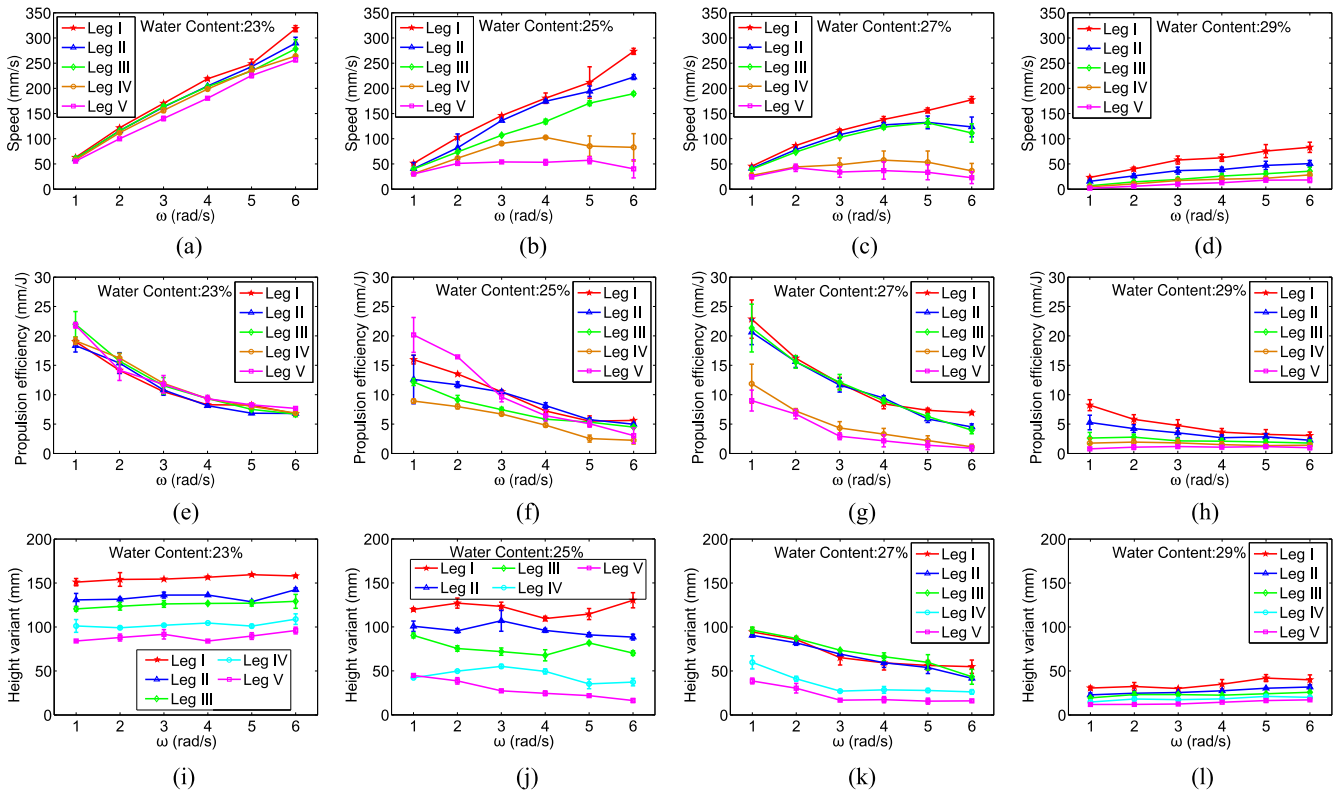
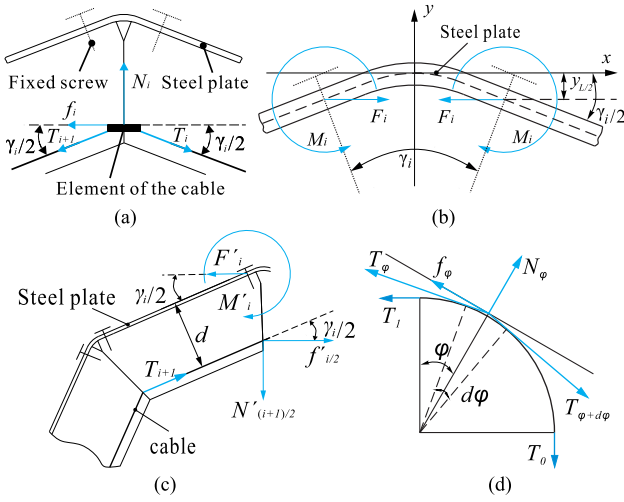


Fig. 6. Experimental results related to the locomotory performance of the two-legged free walking model.

content level and Leg I in 27% water content level, which kept increasing along with the angular velocity. For Leg V in 25% water content level and Legs IV, V in 27% water content level, the forward speed dropped dramatically compared with that of the other legs. However, for Leg IV in 25% water content level and Legs II, III in 27% water content level, the forward speed increased at first and then decreased at a higher angular velocity, meaning that the forward speed had an optimal angular velocity. The experimental result indicates that the mud with the 25% and 27% water content level were more like a non-Newtonian fluid. Their viscosity coefficient changed along with the velocity of the legs moving in the mud. A higher angular velocity might have led to a lower viscous force and a lower propulsion force. Fig. 6(e)–(h) displays the dynamics of the propulsive efficiency of the two-legged model during amphibious locomotion. The following conclusions can be obtained based on the figures. First, the straight legs (Legs I, II, and III) achieved higher propulsive efficiencies than the other legs when the water content level was at 27%. This was not the case when the water content level was lower (23% and 25%), which implies that the propulsive efficiency had a weak relationship with the leg types when the water content was low. When the water content level was highest (29%), the propulsive efficiencies dropped dramatically. Second, the propulsive efficiency generally decreased along with the increase in angular velocity of the legs. This indicates that a lower rotation speed of the curved legs might have achieved a high propulsive efficiency when locomoting in a soft muddy substrate. However, the trend became weak when the water content level was highest (29%). Fig. 6(i)–(l) displays the dynamics of the height variant of the two-legged walking

model, and reveal the following findings. First, the height variant of the two-legged walking model remained stable when the water content level was at 23% and 29%, and decreased slightly along with the increase in angular velocity of the curved legs when the level was at 25% and 27%. Second, the height variant decreased from the straight legs to bent legs. Moreover, the height variant of the walking model decreased along with the increase in water content. When the water content level was at 29% and the mud was more like a thick fluid, the height variant was very small, indicating that the walking model always made contact with the muddy surface during locomotion. The successive contact also increased the drag force acted on the robot, which decreased locomotion speed and propulsion efficiency of the locomotion. For a harder substrate such as mud with a water content level of 23%, the height variant was large, indicating that the walking was unstable.

In summary, Legs I, II, and III were better when the amphibious robot encountered a “softer” substrate based on its locomotion speed and propulsion efficiency. A straighter leg might have pushed away more substrate materials when it engaged in littoral locomotion. However, when the straighter leg walked on hard terrain, the rotation of the curved leg might have led to a large height variant in the amphibious robot body, decreasing the stability of the locomotion. Taking these observations together, the leg of shape III, which was the semicircle leg, was a better choice in AmphiHex-I, as little locomotion speed and cost were lost in muddy substrate and walking was more stable on hard ground. Moreover, it was manufactured simply to lend the same curvature to each part of the curved leg, an observation explained in the next section.



**Fig. 7.** Transformation force analysis. (a) Forces on the element of the cable; (b) forces on the steel plate; (c) forces on one segment of the curved leg; and (d) forces after the arc of the head segments.

### E. Transformation Force of the Flipper Leg

In order to realize the transform motion to adapt various environment, transformation force needs to be analyzed in the design of the flipper leg. Transformation force is relevant to the stiffness of the spring steel plate, the distance between the flexible cable and steel plate  $d$ , and the final state of the curved leg. Fig. 7 displays the force analysis of a flipper leg when it is pulled by a cable. According to Fig. 7(a), the static force equilibrium on the element of the cable between two adjacent segments can be expressed by the following equations:

$$\begin{cases} T_{i+1} \cos(\gamma_i/2) + f_i - T_i \cos(\gamma_i/2) = 0 \\ (T_{i+1} + T_i) \sin(\gamma_i/2) - N_i = 0 \\ f_i = \mu N_i \end{cases} \quad (3)$$

where  $T_i$  and  $T_{i+1}$  denote the force of the cable on the element before and after the  $i$ th joint between two adjacent segments, respectively.  $N_i$  and  $f_i$  denote the normal and friction forces that the leg segments apply on the element, respectively.  $\mu$  denotes the friction coefficient between the cable and segments.  $\gamma_i$  denotes the angle between two adjacent segments. Based on the preceding equations, we can obtain the relationship between  $T_i$  and  $T_{i+1}$  as follows:  $T_i/T_{i+1} = (1 + \mu \tan(\gamma_i/2))/(1 - \mu \tan(\gamma_i/2))$ .

Fig. 7(b) displays the steel plate force analysis. If the steel plate is simplified to a beam, we find the following:

$$\frac{d^2 y}{dx^2} = -\frac{F_i(y - y_{L/2}) + M_i}{EI} \quad (4)$$

where  $E$  and  $I$  denote the elastic modulus and inertia moment of the steel plate, respectively.  $y$  denotes the deflection of the beam.  $F_i$  and  $M_i$  denote the force and torque that the fixed screws apply on the beam, respectively. We can obtain the following equation from the following boundary conditions:  $(F_i \gamma_i)/(2M_i) - (2\pi/K_i) \tan(2\pi L/(2K_i)) = 0$ , where  $K_i$  can be obtained by  $(2\pi/K_i)^2 = F_i/EI$ .

Considering the static force and torque equilibrium of the segment in Fig. 7(c), we find the following:

$$\begin{cases} T_{i+1} \cos(\gamma_i/2) + f_i - F_i = 0 \\ T_{i+1} \sin(\gamma_i/2) - N'_{(i+1)/2} = 0 \\ f'_{(i+1)/2} = \mu N_{(i+1)/2} \end{cases} \quad (5)$$

and

$$\begin{cases} T_{i+1} d + \frac{f_{i/2} d}{\cos(\gamma_i/2)} - M_i = 0 \\ \frac{F'_i d}{\cos(\gamma_i/2)} - M_i = 0 \end{cases} \quad (6)$$

where  $N'_{(i+1)/2}$  and  $f'_{(i+1)/2}$  are the normal and friction forces that the cable element applies on the  $(i+1)$ th segment, respectively.  $F_i$  and  $M_i$  are the steel plate forces on the segment. We can obtain the force of the cable on the head segment  $T_1$  by combining the preceding equations as follows:

$$T_1 = \frac{(2\pi/K_n)^2 EI}{\cos(\gamma_n/2) + \mu \sin(\gamma_n/2)} \prod_{i=1}^n \left( \frac{1 + \mu \tan(\gamma_i/2)}{1 - \mu \tan(\gamma_i/2)} \right) \quad (7)$$

where  $n$  denotes the number of joints. Because the cable runs through an arc to connect the driving module as shown in Fig. 7(d), the force that the connecting shaft should provide  $T_0$  can be calculated according to

$$\begin{cases} T_\phi + f_\phi - T_{\phi+d\phi} = 0 \\ T_\phi \sin(d\phi/2) + T_{\phi+d\phi} \sin(d\phi/2) \simeq 2T_\phi \phi/2 = N_\phi \\ f_\phi = \mu N_\phi \end{cases} \quad (8)$$

where  $T_\phi$  denotes the force at the element with angle  $\phi$ . From the equations, we could obtain that  $T_0 = T_1 e^{\mu \Delta\phi}$ , where  $\Delta\phi$  denotes the angle at which the cable turns around.

The diameter and pitch of the screw are 12 and 2 mm, respectively. The translational distance of the cable that pulls the leg from straight to circled status  $L_s$  can be calculated as  $L_s = 2nd \tan(\gamma/2)$ , which is about 16 mm. We assume that the friction coefficient between the screw (40 Cr) and nut (copper) is 0.1. Considering the power of the robot and the requested transform force, we adopt a 12-V/0.7-W dc motor as the transformation motor, which can provide a 0.087-N·m torque to the screw pair, and a 63-N pulling force on the first segment of the flipper leg. The transformation of the flipper leg can be finished within 3 s.

Assuming that all of the joints reach their maximum bending angles, the transformation forces in related to the thickness of the steel plate and the leg shape are shown in Fig. 8(a) and (b), respectively. From the figure, we could obtain that Legs I and III provide lower requirements for the transformation force, and a 0.2 mm thickness steel plate is suitable for the transform motor with a considerable stiffness during swimming. In summary, Leg III is suitable for AmphiHex-I for its effectiveness of the locomotion in muddy terrains and easy manufactured with the same  $\gamma_i$  for each segment.

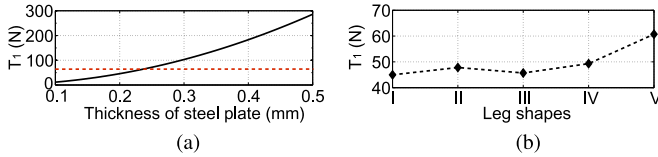


**Fig. 8.** Transformation force of the flipper leg. (a) Transformation force  $T_1$  with regard to the thickness of the steel plate, a 65-Mn quenched spring steel plate is used, the distance between the flexible cable and steel plate  $d$  is set at 5 mm, and Leg III is adopted for calculation. The horizontal red line denotes the maximum transform force that the transform motor could provide. (b) Transformation force  $T_1$  with regard to leg types, the thickness of the steel plate is set at 0.2 mm.

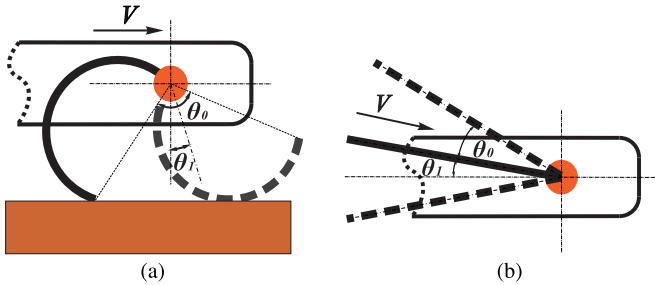


**Fig. 9.** Motion of the flipper leg. (a) Kinematic parameters during rotation, usually occupied in a curved leg; (b) kinematic parameters during oscillation, usually occupied in a straight flipper.

### III. GAIT AND GAIT TRANSITION FOR AMPHIBIOUS LOCOMOTION

Despite the Leg shapes, properties of muddy substrate, and kinematic parameters of single leg, gaits and gait transition are also very important for the locomotion of AmphiHex-I in littoral environment. A gait is a periodic pattern of coordinated movement made by several flipper legs during locomotion. Thanks to the transformable flipper-leg propulsion mechanisms, AmphiHex-I can rely on versatile gaits to adapt to complex environments.

#### A. Flipper-Leg Kinematic Parameters

The motion of a single flipper leg is the foundation of a gait. The flipper leg makes two kinds of motions: transformation and propulsion. Transformation can be accomplished using the transformation motor when the flipper leg locates a predefined position. As for propulsion, two modes basically correspond to two states of the flipper leg. When the flipper leg is in its curved state, it rotates to propel AmphiHex-I to walk on terrains, as illustrated in Fig. 9(a). When the flipper leg is in its straight state, it oscillates to propel AmphiHex-I to swim underwater, as illustrated in Fig. 9(b). According to Fig. 9(a), the rotation-related kinematic parameters of flipper legs include  $\omega_s$ ,  $\omega_t$ ,  $\theta_0$ , and  $\theta_1$ , where  $\theta_0$  denotes the size of the region from where the curved leg makes contact with the substrate to where it leaves the substrate. This can be considered the supportive stage, with the region beyond it classified as a transition stage.  $\theta_1$  denotes the phase position of the supportive stage, and is defined as the angle from the center of the region to the vertical line. AmphiHex-I usually adopts a tripod gait to walk on land, which means that

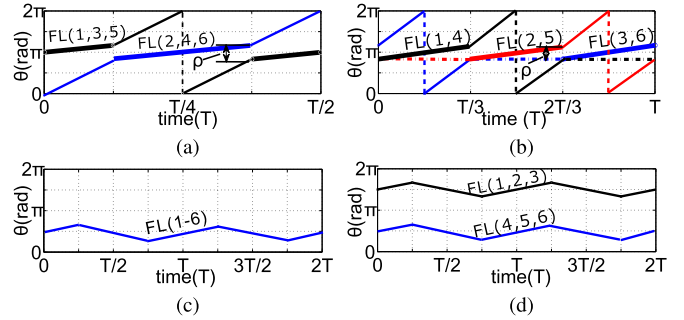


**Fig. 10.** Trajectory of AmphiHex-I gait. (a) Trajectory of tripod gait. The blue and black lines denote the two groups of the tripod, respectively. The bold line denotes supportive stage, and the regular line denotes the transition stage,  $C = [0, 0.5, 0, 0.5, 0, 0.5]$ . (b) Trajectory of tetrapod gait,  $C = [0, 0.33, 0.67, 0, 0.33, 0.67]$ . The dashdot lines denote the waiting stage. (c) Trajectory of cruising gait underwater,  $A = [\pi/2, \pi/2, \pi/2, \pi/2, \pi/2, \pi/2]$ . (d) Trajectory of turning gait underwater,  $A = [\pi/2, \pi/2, \pi/2, 0, 0, 0]$ .

the six legs can be classified into two groups. To decrease the fluctuation of the robot, one group of legs should enter the supportive stage when the other group of legs leaves it, instituting the same timespan for the two stages. However, the supportive stage is often smaller than the transition stage, which means that the rotation speed of the leg in the supportive stage  $\omega_s$  is larger than that in the transition stage  $\omega_t$ . The rotation period  $T$  can be calculated as  $T = \theta_1/\omega_s + (2\pi - \theta_1)/\omega_t$ . Fig. 9(b) presents the kinematic parameters of the flipper leg oscillating underwater. The kinematic parameters that describe the oscillation of the flipper leg include  $\theta_0$ ,  $\theta_1$ , and  $T$ , where  $\theta_0$  denotes the flipper's oscillation amplitude and  $\theta_1$  denotes its propulsion direction, calculated from the vertical line to the center of the oscillation.  $T$  denotes the oscillation period.

#### B. Gaits for Terrestrial and Underwater Locomotion

By combining the flipper leg's various motions, AmphiHex-I may possess versatile gaits that make the robot adaptable to different environments. Each gait has its advantages in a specific environment. Before defining the gaits, we label the left-fore, left-middle, left-rear, right-fore, right-middle, and right-rear flipper legs as flipper legs 1–6 (FL1–6), respectively. The key parameter to forming a gait is the coordinate parameter, which can be expressed by a vector,  $C = [0, \rho_2, \rho_3, \rho_4, \rho_5, \rho_6]$ , where  $\rho_i$  denotes the phase difference when the  $i$ th flipper leg begins its supportive stage compared with flipper leg 1.

AmphiHex-I usually uses a tripod gait for various rough terrains. For the tripod gait, flipper legs 1, 3, and 5 form one group, and flipper legs 2, 4, and 6 form another group. The movement of flipper legs in the same group is synchronous, and the two groups exhibit a phase difference. When one group of legs enters the supportive stage, the other group is entering the transition stage. Fig. 10(a) presents an example of the trajectory of the tripod gait. The tripod gait leads to a high locomotion speed with a relative stable posture, which is not only suitable for terrestrial locomotion but also for soft substrates such as sandy and muddy terrain. Diagonal gait is analogous to tripod gait, except that flipper legs 1, 2, 6 and 3, 4, 5 form two groups, respectively. However, if the leg movements are classified into three groups,

indicating that the rotation of the two forelegs, two median legs, and two rear legs are synchronous, respectively, then the gait is a tetrapod gait. Due to its synchronous rotation of legs in the same location along the longitudinal line of the body, a tetrapod gait is suitable for climbing stairs or slopes. Fig. 10(b) presents the trajectory of the tetrapod gait.

With six propulsion flippers oscillating as vectored thrusters, AmphiHex-I has versatile swimming maneuvers underwater. In a swimming gait, there is a vectoring parameter  $A = [\theta_{11}, \theta_{12}, \theta_{13}, \theta_{14}, \theta_{15}, \theta_{16}]$ .  $\theta_{1i}$  denotes the propulsion direction of flipper leg  $i$ . The six flippers of AmphiHex-I possess the same  $\theta_1 = \pi/2$  in the cruising gait, as presented in Fig. 10(c). However, in the turning gait,  $A$  is defined as  $[0, 0, 0, \pi/2, \pi/2, \pi/2]$ , which means that the left three flippers oscillate in one direction, while the other three oscillate in the opposite direction, the gait trajectory is shown in Fig. 10(d). When the six flippers oscillate in the same up-and-front direction, the robot engages in a rising motion, where  $A = [\pi/3, \pi/3, \pi/3, \pi/3, \pi/3, \pi/3]$ . When the six flippers adopt a coordinated thrusting direction, the robot can also perform maneuvers such as sinking, breaking, rolling, and retreating. An underwater gait transition is usually simple. Changing the vectoring parameter  $A$  produces various swimming gaits during an underwater transition.

### C. Gait for Littoral Locomotion

In addition to the tripod and tetrapod gaits, AmphiHex-I can adopt some special gaits for locomotion in littoral areas, especially for muddy terrain. For example, when its six legs rotate synchronously, AmphiHex-I walks with a hexapod gait, with a coordinated parameter of  $[0, 0, 0, 0, 0, 0]$ . If the hexapod gait is used during locomotion on hard terrain, the height variant of the robot is relatively large and the impact on the robot is also high. However, if AmphiHex-I walks on a soft muddy substrate, the legs sink into the mud easily and the body of the robot may make contact with the substrate. At this time, the robot provides a larger propulsion force with a hexapod gait to help alleviate the situation. The robot's fluctuation in the vertical direction is also small according to the experimental results in Section II-C. Moreover, AmphiHex-I can use its transformable structure to enhance its ability to free itself when it becomes stuck. When the curved legs transform into straight flippers, rotating the flippers pushes away more muddy materials, making the reaction force of the flipper legs higher than that exerted by the rotation of the rigid curved legs.

It is important for field robots to adapt to different environments and make smooth transitions between different substrates. Gait transition can be a coordinated movement of legs or a change in state of the flipper legs, which may occur at the beginning, middle, or end of a gait. AmphiHex-I may adopt a tripod gait to obtain a high locomotion speed in muddy terrain. However, when it comes to a softer muddy substrate with a higher water content level, the robot may sink and be trapped in muddy substrate for the lack of supportive and forward propulsive force. In this situation, the robot could transit its gait from tripod gait to hexapod gait to alleviate the straits. Fig. 11 displays two examples of the tripod-to-hexapod gait transition. In Fig. 11(a), left and right tripods are transitioned into hexapod with synchronous motion. A waiting stage is added to change the

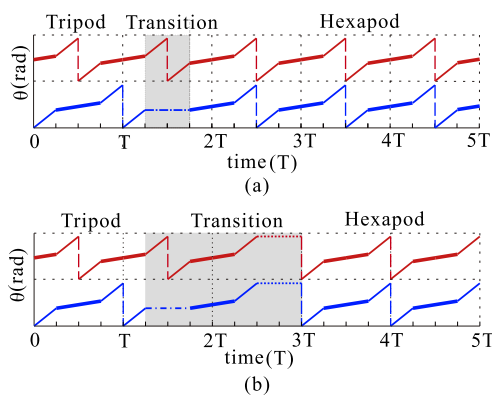


Fig. 11. Tripod-to-Hexapod gait transition. The red and blue lines denote the left and the right tripod, respectively. The dotted line denotes the transformation process, and the dashdot line denotes the waiting process during transition. (a) Trajectory of tripod to hexapod gait; (b) trajectory of tripod to hexapod gait with straight flippers.

phase difference of the flipper legs while maintaining a stable stance. In Fig. 11(b), the tripod gait is transitioned to hexapod gait with straight flippers, which involves transformation stages. In order to avoid interference, the transformation occurs when the curved legs are in transition phase, that is  $\theta = 2\pi$ .

### D. Gait for Environment Transition

Besides terrestrial, littoral, and swimming gaits, the robot can combine the two states of its flipper legs to adopt a hybrid gait. During the transition between land and water, part of the robot remains buoyant in water, while the other part makes contact with soft substrate. The robot may correspondingly adopt a hybrid gait in which its straight flippers oscillate underwater and its curved legs rotate on the muddy substrate. For example, in a landing motion, when a robot swims close to the slope of shore-side substrate, its two front flippers transform into curved legs. The middle and rear flippers continue to oscillate to generate a propulsion force for the robot, which also increases the locomotive effectiveness of the two curved forelegs. In this case, AmphiHex-I transforms more of its flippers into legs and uses a hybrid gait to perform an environment transition. This transformation takes place only in water to ensure the robot's standing stability on land. In other words, the transformation motion from curved legs to straight flippers or from straight flippers to curved legs is conducted underwater.

Fig. 12 presents an example of environment transition. When AmphiHex-I enters into water, it adopts a tripod gait initially. The robot's six legs stop at a certain position, then its two forelegs transform into straight flippers and oscillate to provide propulsion. The middle legs and rear legs also transform successively later. Finally, AmphiHex-I adopts various swimming gaits underwater, and performs a gait transition during its landing process. Throughout the transition, the two states of the flipper legs ensure effective propulsion in different environments. In areas between water and land, such as shoal, shallow water, and wet land, AmphiHex-I has a big advantage because its six flipper legs can be controlled independently between their curved and straight states.

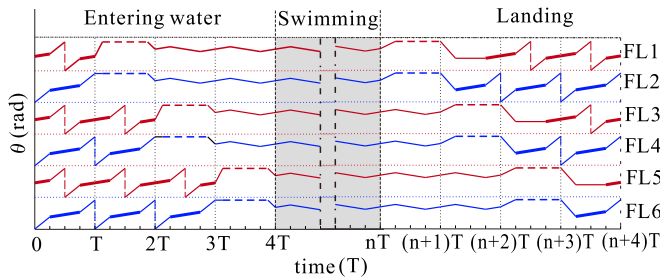


**Fig. 12.** Leg trajectories of AmphiHex-1 with hybrid gait and gait transition. It first adopts a tripod gait (0– $T$ ), then the curved legs transform into straight flippers successively from front legs to rear legs ( $T$ – $4T$ ). It could swim with straight flippers after all the bodies of the robot entering water ( $4T$ – $nT$ ). When landing, AmphiHex-1 will adopt hybrid gait again and transform the straight flippers into curved legs according to the landing progress ( $nT$ – $(n+4)T$ ).

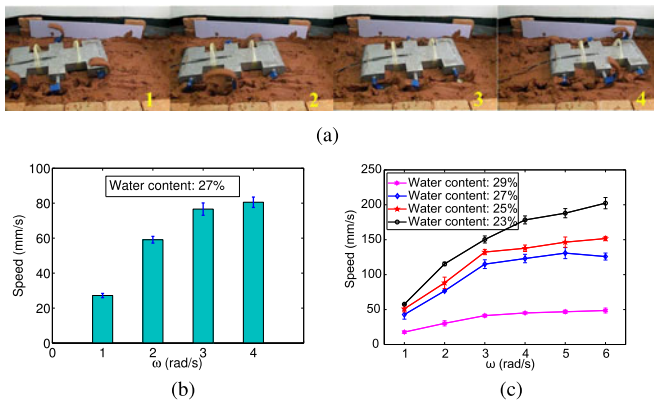


**Fig. 13.** AmphiHex-1 in muddy substrate. (a) Snapshots of the robot adopting a tripod gait in muddy substrate; (b) locomotion speed with tripod gait, where  $\theta_0 = 60^\circ$ ; (c) locomotion speed with hexapod gait, where  $\omega = \omega_s = \omega_t$ .

#### IV. EXPERIMENTS AND RESULTS

We conducted massive outdoor locomotion experiments on various substrates to validate the effectiveness of AmphiHex-I's transformable flipper legs and locomotory performance. In most situations, the substrates were natural, providing the robot with more realistic environments.

##### A. Locomotion in a Littoral Environment

We prepared a littoral environment to test the locomotion of AmphiHex-I by gathering mud from a river bed. Similar to the two-legged free walking experiment, we conducted a series of experiments to test the robot's locomotory performance in terms of its various leg speeds and kinematic parameters. Snapshots of AmphiHex-I walking in muddy substrate and the robot's speed when adopting various gaits are presented in Fig. 13 (a)–(c), respectively. Fig. 13(b) reveals that the locomotion speed of the robot with a tripod gait was relatively low in muddy substrate. The speed of the robot increased as the angular velocity of the legs increased. However, the trend became weak when the rotation speed of the legs was high, implying that the legs had an optimal angular velocity during locomotion in the muddy substrate. Fig. 13(c) indicates that the propulsion speed of AmphiHex-I when it adopted a hexapod gait was much

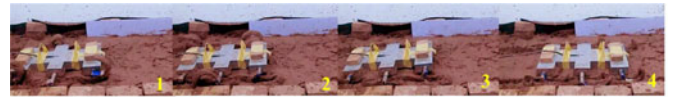


**Fig. 14.** Snapshots of AmphiHex-1 extricating itself from muddy terrain via gait transition (see movie). (1) and (2): AmphiHex-1 adopts a tripod gait, which decreases its speed. Note that the robot has an extra load of about 3 kg. (3) and (4): AmphiHex-1 transitions to a hexapod gait to effectively pass through the muddy substrate.

higher than that of the robot with a tripod gait. In fact, the robot's tripod gait produced a higher locomotion speed than its hexapod gait on hard terrains and vice versa on soft muddy terrain. This indicates that the robot might have transformed its tripod gait into a hexapod gait to free itself. From the figure, we can also conclude that there exists an optimal rotating speed of the flipper legs for a higher locomotion speed in muddy substrates with 25% and 27% water content levels. When the water content level is at 29%, the locomotion speed dropped dramatically. These results coincide with the results of the two-legged free walking experiment conducted in Section II-C, which also validates the effectiveness of the walking model. Note that in the hexapod gait adopted here, the rotating speed of the flipper leg kept constant.

When the robot sinks into mud, it can adopt two extrication methods. First, it can transition its tripod gait into a hexapod gait. Second, it can loosen the cable and transform its rigid curved legs into flexible straight flippers and walk using a hexapod gait. The robot may push more mud when adopting a hexapod gait with curved legs. However, considering that a flexible flipper leads to a slower shear speed and larger reacting, forwarding and supporting forces, adopting a hexapod gait with straight flippers may also be an effective extrication method. Fig. 14 presents a series of snapshots of the robot adopting gait transitions to extricate itself from muddy terrain.

##### B. Environment Transition With Hybrid Gaits

Environment transition of Amphibious robot includes landing from water and entering water from land. Doing both effectively is a challenging task. AmphiHex-I can do so easily thanks to its transformable flipper-leg composite propulsion mechanisms and its unique hybrid gait, especially in a totally natural environment such as a soft muddy shore. Fig. 12 presents the trajectories of the robot's flipper legs during its locomotion between water and land via its use of hybrid gaits and gait transitions. We conducted the landing experiment at a natural lake with a muddy gradient shore. Fig. 15 presents a series of snapshots of AmphiHex-I performing the landing motion, and shows that it successfully transitioned from the water to land. During the landing process, the robot adopted a swimming gait, a hybrid gait with different flippers and legs, a hexapod gait, and a diagonal gait to adapt to the complex amphibious environments. Note that the transition in the experiment was triggered manually instead of being triggered by sensors. Even so, the robot still exhibited very strong adaptive ability on the complex environment transition. To our knowledge, it was the first time for an amphibious robot to land on such a natural and formidable muddy bank, which validated the effectiveness of the transformable flipper leg and the corresponding gaits.

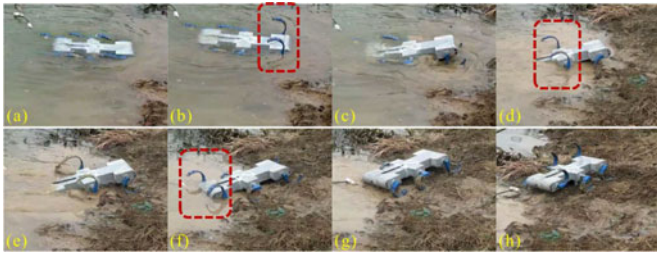


**Fig. 15.** Snapshots of AmphiHex-I during landing with hybrid gaits and gait transition [see movie]. (a) Cruising with swimming gait; (b) two fore flippers transforming into legs; (c) a hybrid gait with two legs and four flippers; (d) two middle flippers transforming into legs; (e) a hybrid gait with four legs and two flippers; (f) two rear flippers transforming into legs; (g) climbing muddy terrain with a hexapod gait; (h) climbing a slope with a diagonal gait.

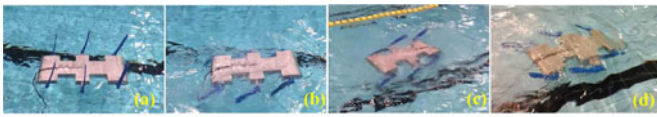


**Fig. 16.** AmphiHex-I maneuvers underwater: (a) standby; (b) cruising; (c) turning; (d) diving.

### C. Underwater Locomotion

Given that its six flippers function as vectored thrusters, AmphiHex-I has plenty of maneuvering actions underwater. Fig. 16 presents a series of aquatic movements performed by AmphiHex-I in a swimming pool with a depth of 1.5 m. AmphiHex-I adopted a standby position with its six flippers perpendicular to its body in the same direction, and cruised by oscillating its six flippers near to its body at a speed of approximately half its body length per second [see Fig. 16(b)]. It also accomplished movements like braking by keeping its six flippers perpendicular to the body, rolling by oscillating the three flippers perpendicular to each side of the body in opposite directions, pivot steering by oscillating the flippers parallel to the body on one side with the flippers on the other side oscillating in an opposite direction [see Fig. 16(c)], diving by oscillating the six flippers upward simultaneously [see Fig. 16(d)], and ascending by oscillating the six flippers downward simultaneously. The locomotion speed of AmphiHex-I underwater is about 0.2 m/s with a cruising gait ( $\theta_0 = 20^\circ$ ,  $T = 0.5$  s). The locomotion speed showed positive correlation with the oscillation amplitude and the oscillation frequency of the flippers.

### D. Climbing Slopes and Stairs

Besides the locomotion in muddy terrain and underwater, we also validated the capability of AmphiHex-I to climb slopes and stairs via experiments. Fig. 17(a) illustrates AmphiHex-I walking on slopes and stairs. Fig. 17(b) and (c) displays the change in the robot's locomotion speed on slopes and stairs with different gradients, respectively. The figures indicate that the robot's locomotion speed on a slope decreased along with the increase in the slope's gradient, and that the tripod gait with  $\theta_1 = 15^\circ$  led to a higher locomotion speed. When the gradient slope was  $30^\circ$ , the robot adopted a tripod gait with  $\theta_1 = 0^\circ$  and failed to climb the slope. The robot could not climb any

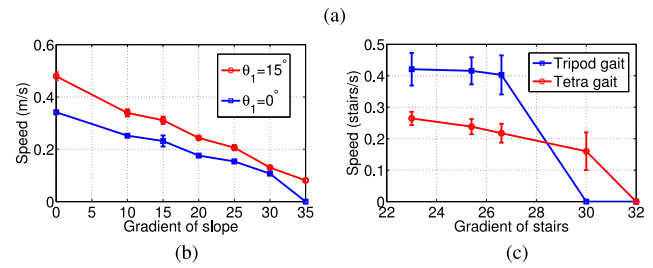


**Fig. 17.** AmphiHex-I climbing slope and stairs: (a1) climbing a slope with a tripod gait,  $\theta_1 = 15^\circ$ ; (a2) climbing a slope with a tripod gait,  $\theta_1 = 0^\circ$ ; (a3) climbing stairs with a tetrapod gait and (a4) climbing stairs with a tripod gait; (b) locomotion speed on slopes; (c) locomotion speed on stairs.

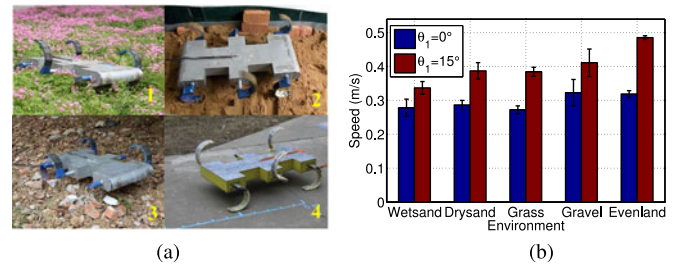


**Fig. 18.** AmphiHex-I's locomotion on various rough terrains: (a) grass (1), wet sand (2), gravel (3) and even ground (4); (b) locomotion speed on various terrains.

slope with a gradient more than  $35^\circ$  regardless of the gait and kinematic parameters adopted. The robot adopted two kinds of gaits when climbing stairs: tripod and tetrapod. According to the experiment results, the tripod gait might have led to a change in the locomotion direction by making the two parallel legs nonsynchronous and increasing the speed of the robot. However, the tetrapod gait might have improved the robot's stability given an unchanging velocity direction and a higher locomotion speed when the stairs were steeper.

### E. Locomotion on Rough Terrains

In addition to the strong adaptive ability to amphibious environments, the robot can also perform terrestrial locomotion effectively. We also tested AmphiHex-I's terrestrial locomotion capability on various rough terrains, as shown in Fig. 18(a) and (b). Fig. 18(b) displays the locomotion speed of AmphiHex-I on various terrains with different kinematic parameters  $\theta_1$ . In the experiment, we set  $\theta_0$  at  $60^\circ$ . When  $\theta_1$  was zero, the robot was more stable with a small fluctuation in the body. However, when  $\theta_1$  increased, the supportive stage arrived earlier, which benefited the robot's locomotion when climbing a slope and harmed its locomotion on flat ground due to a large fluctuation in the body. However, a larger  $\theta_1$  (set at  $15^\circ$  in the experiment) led to a high locomotion speed on various terrains, as shown in

Fig. 18(b). The reason lies in that the robot's inertia was utilized in the locomotion with a higher  $\theta_1$ .

## V. CONCLUSION AND FUTURE WORK

In this paper, we have presented a detailed study on the locomotory performance of AmphiHex-I in amphibious environments. Given its especially designed transformable flipper legs and versatile gaits, AmphiHex-I has a strong locomotion ability on rough terrains, in littoral areas and underwater. After analyzing the influence of the kinematic parameters, the properties of soft substrates and the shape of curved legs on locomotory performance, we conducted experiments to consider its locomotion on various natural terrains. The results validate the effectiveness of the designed transformable flipper-leg mechanisms and AmphiHex-I overall.

The transformable flipper-leg propulsion mechanism has several great advantages in an amphibious robot. First, the flipper leg is a composite propulsion that can propel a robot underwater and on rough terrains simultaneously, decreasing its weight and improving its efficiency. The robot can use two effective locomotion mechanisms on rough terrains and underwater that have been validated by RHex and AQUA series robots. Second, the transformation of the flipper leg is very simple and effective. The hybrid gait and gait transition in the field experiments have verified the effectiveness of the mechanisms. Third, the combination of the flipper legs' different states facilitates AmphiHex-I's amphibious behaviors. In current design, one cable runs through the center of the flipper leg. Literal forces on the flipper leg during locomotion on rough terrains increase the wear and tear of the leg segments and the steel plate. The problem can be solved through using two cables in parallel to pull the flipper leg.

Future work should include the following aspects. First, the theoretical model on the dynamics of flipper legs during pushing soft muddy substrates should be established to acquire a deeper understanding of the complex physics associated with the interaction between propulsion devices and environmental media. Second, the influence of the stiffness of the flipper leg on the locomotory performance in muddy terrain and underwater should be investigated thoroughly. Third, the autonomous selection and transition of the gaits of the robot in various environments should be incorporated through equipping related sensors and designing suitable controlling algorithm.

## ACKNOWLEDGMENT

The authors would like to thank X. Ren, H. Huang, Z. Kong, X. Wang, P. Liu, and L. Xu for their help in setting up the experimental platform and in conducting the experiments.

## REFERENCES

- [1] M. H. Dickinson, C. T. Farley, R. J. Full, M. A. R. Koehl, R. Kram, and S. Lehman, "How animals move: An integrative view," *Science*, vol. 288, pp. 100–106, Apr. 2000.
- [2] J. A. Clack, "The fin to limb transition: New data, interpretations, and hypotheses from paleontology and developmental biology," *Annu. Rev. Earth Planet. Sci.*, vol. 37, no. 1, pp. 163–179, 2009.
- [3] T. M. Lejeune, P. A. Willems, and N. C. Heglund, "Mechanics and energetics of human locomotion on sand," *J. Exp. Biol.*, vol. 201, no. 13, pp. 2071–2080, 1998.
- [4] D. Ferris, M. Louie, and C. Farley, "Running in the real world: Adjusting the leg stiffness for different surfaces," *Proc. Biol. Sci.*, vol. 265, pp. 989–994, Apr. 1998.
- [5] R. D. Maladen, D. Yang, P. B. Umbanhowar, A. Kamor, and D. I. Goldman, "Mechanical models of sandfish locomotion reveal principles of high performance subsurface sand-swimming," *J. Roy. Soc. Interface*, vol. 8, no. 62, pp. 1332–1345, 2011.
- [6] R. D. Maladen, D. Yang, L. Chen, and D. I. Goldman, "Undulatory swimming in sand: Subsurface locomotion of the sandfish lizard," *Science*, vol. 325, no. 5938, pp. 314–318, 2009.
- [7] L. Chen, P. B. Umbanhowar, H. Komsuoglu, D. E. Koditschek, and D. I. Goldman, "Sensitive dependence of the motion of a legged robot on granular media," *Proc. Nat. Acad. Sci.*, vol. 106, no. 9, pp. 3029–3034, 2009.
- [8] G. Dudek, P. Giguere, C. Prahacs, S. Saunderson, J. Sattar, L. Torres-Mendez, M. Jenkin, A. German, A. Hogue, A. Ripsman, J. Zacher, E. Milios, H. Liu, P. Zhang, M. Buehler, and C. Georgiades, "Aqua: An amphibious autonomous robot," *Computer*, vol. 40, no. 1, pp. 46–53, Jan. 2007.
- [9] J. Yu, R. Ding, Q. Yang, M. Tan, W. Wang, and J. Zhang, "On a bio-inspired amphibious robot capable of multimodal motion," *IEEE/ASME Trans. Mechatronics*, vol. 17, no. 5, pp. 847–856, Oct. 2012.
- [10] A. Crespi, K. Karakasiliotis, A. Guignard, and A. Ijspeert, "Salamandra Robotica II: An amphibious robot to study salamander-like swimming and walking gaits," *IEEE Trans. Robot.*, vol. 29, no. 2, pp. 308–320, Apr. 2013.
- [11] J. Yu, R. Ding, Q. Yang, M. Tan, and J. Zhang, "Amphibious pattern design of a robotic fish with wheel-propeller-fin mechanisms," *J. Field Robot.*, vol. 30, no. 5, pp. 702–716, 2013.
- [12] A. J. Ijspeert, A. Crespi, D. Ryczko, and J.-M. Cabelguen, "From swimming to walking with a salamander robot driven by a spinal cord model," *Science*, vol. 315, no. 5817, pp. 1416–1420, 2007.
- [13] A. Crespi and A. Ijspeert, "Online optimization of swimming and crawling in an amphibious snake robot," *IEEE Trans. Robot.*, vol. 24, no. 1, pp. 75–87, Feb. 2008.
- [14] A. Carlson and N. Papanikolopoulos, "Aquapod: Prototype design of an amphibious tumbling robot," in *Proc. IEEE Int. Conf. Robot. Autom.*, May 2011, pp. 4589–4594.
- [15] Y. Sun and S. Ma, "epaddle mechanism: Towards the development of a versatile amphibious locomotion mechanism," in *Proc. IEEE/RSJ Int. Conf. Intell. Robots Syst.*, 2011, pp. 5035–5040.
- [16] B. Dey, S. Manjanna, and G. Dudek, "Ninja legs: Amphibious one degree of freedom robotic legs," in *Proc. IEEE Int. Conf. Intell. Robots Syst.*, Nov. 2013, pp. 5622–5628.
- [17] V. Kaznov and M. Seeman, "Outdoor navigation with a spherical amphibious robot," in *Proc. IEEE Int. Conf. Intell. Robots Syst.*, Oct. 2010, pp. 5113–5118.
- [18] H. Kim, D. G. Lee, K. Jeong, and T. Seo, "Water and ground-running robotic platform by repeated motion of six spherical footpads," *IEEE/ASME Trans. Mechatronics*, to be published.
- [19] R. Harkins, J. Ward, R. Vaidyanathan, A. Boxerbaum, and R. Quinn, "Design of an autonomous amphibious robot for surf zone operations: Part II—Hardware, control implementation and simulation," in *Proc. IEEE/ASME Int. Conf. Adv. Intell. Mechatron.*, Jul. 2005, pp. 1465–1470.
- [20] A. Boxerbaum, P. Werk, R. Quinn, and R. Vaidyanathan, "Design of an autonomous amphibious robot for surf zone operation: Part I. Mechanical design for multi-mode mobility," in *Proc. IEEE/ASME Int. Conf. Adv. Intell. Mechatron.*, Jul. 2005, pp. 1459–1464.
- [21] S. Hirose and H. Yamada, "Snake-like robots machine design of biologically inspired robots," *IEEE Robot. Autom. Mag.*, vol. 16, no. 1, pp. 88–98, Mar. 2009.
- [22] X. Liang, M. Xu, L. Xu, P. Liu, X. Ren, Z. Kong, J. Yang, and S. Zhang, "The AmphiHex: A novel amphibious robot with transformable leg-flipper composite propulsion mechanism," in *Proc. IEEE Int. Conf. Intell. Robots Syst.*, 2012, pp. 3667–3672.
- [23] S. Zhang, X. Liang, L. Xu, and M. Xu, "Initial development of a novel amphibious robot with transformable fin-leg composite propulsion mechanisms," *J. Bionic Eng.*, vol. 10, no. 4, pp. 434–445, 2013.
- [24] S. Seok, A. Wang, M. Y. M. Chuah, D. J. Hyun, J. Lee, D. M. Otten, J. H. Lang, and S. Kim, "Design principles for energy-efficient legged locomotion and implementation on the MIT cheetah robot," *IEEE/ASME Trans. Mechatronics*, vol. 20, no. 3, pp. 1117–1129, Jun. 2015.
- [25] U. Saranli, M. Buehler, and D. Koditschek, "Design, modeling and preliminary control of a compliant hexapod robot," in *Proc. IEEE Int. Conf. Robot. Autom.*, 2000, pp. 2589–2596.

- [26] U. Saranlı, M. Buehler, and D. Koditschek, "Rhex: A simple and highly mobile hexapod robot," *Int. J. Robot. Res.*, vol. 20, no. 7, pp. 616–631, 2001.
- [27] M. Triantafyllou and G. Triantafyllou, "An efficient swimming machine," *Sci. Amer.*, vol. 272, pp. 64–70, 1995.
- [28] C. Zhou and K. H. Low, "Design and locomotion control of a biomimetic underwater vehicle with fin propulsion," *IEEE/ASME Trans. Mechatronics*, vol. 17, no. 1, pp. 25–35, Feb. 2012.
- [29] Q. Yan, Z. Han, S. Zhang, and J. Yang, "Parametric research of experiments on a carangiform robotic fish," *J. Bionic Eng.*, vol. 5, no. 3, pp. 95–101, 2008.
- [30] Z. Su, J. Yu, M. Tan, and J. Zhang, "Implementing flexible and fast turning maneuvers of a multijoint robotic fish," *IEEE/ASME Trans. Mechatronics*, vol. 19, no. 1, pp. 329–338, Feb. 2014.
- [31] Z. Chen, S. Shatarra, and X. Tan, "Modeling of biomimetic robotic fish propelled by an ionic polymer metal composite caudal fin," *IEEE/ASME Trans. Mechatronics*, vol. 15, no. 3, pp. 448–459, Jun. 2010.
- [32] L. Xu, X. Liang, M. Xu, and S. Zhang, "Interplay of theory and experiment in analysis of the advantage of the novel semi-elliptical leg moving on loose soil," in *Proc. IEEE/ASME Int. Conf. Adv. Intell. Mechatron.*, 2013, pp. 26–31.
- [33] L. Chen, T. Zhang, and D. Goldman, "A terradynamics of legged locomotion on granular media," *Science*, vol. 339, pp. 1408–1412, 2013.
- [34] K. Iagnemma, S. Kang, H. Shibly, and S. Dubowsky, "Online terrain parameter estimation for wheeled mobile robots with application to planetary rovers," *IEEE Trans. Robot. Autom.*, vol. 20, no. 5, pp. 921–927, Oct. 2004.
- [35] R. M. Alexander, *Principles of Animal Locomotion*. Princeton, NJ, USA: Princeton Univ. Press, 2006.



**Shiwu Zhang** (M'12) received the B.S. and Ph.D. degrees from the University of Science and Technology of China (USTC), Hefei, China, in 1997 and 2003, respectively.

He is currently an Associate Professor in the Department of Precision Machinery and Precision Instrumentation at USTC. He has been a Postdoctoral Research Fellow at the Department of Computer Science, Hong Kong Baptist University, Hong Kong. He has authored or coauthored more than 70 technical peer-reviewed

papers. His current research interests include bioinspired robots, terradynamics, and multimodal biomedical imaging.



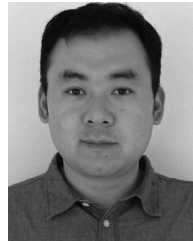
**Youcheng Zhou** received the B.E. degree in mechanical engineering from Hunan Normal University, Changsha, China, in 2009. He is currently working toward the M.S. degree in the Department of Precision Machinery and Precision Instrumentation, University of Science and Technology of China, Anhui, China.

His research interests include amphibious robots, mobile robots, and CPG-based locomotion.



**Min Xu** received the B.E. degree in mechanical engineering from the Hefei University of Technology, Hefei, China, in 1995, and the M.S. degree in mechanical and electrical engineering from the Department of Precision Machinery and Precision Instrumentation, University of Science and Technology of China (USTC), Anhui, China, in 1999.

He is currently a Lecturer in the Department of Precision Machinery and Precision Instrumentation, USTC. He leads research projects focusing on soft robotic arms supported by the National Science Foundation of China. His research interests include intelligent robots, soft robots, and shape memory alloy.



**Xu Liang** received the B.E. degree in mechanical engineering from Northeast Agricultural University, Harbin, China, in 2008, and the Ph.D. degree from the Department of Precision Machinery and Precision Instrumentation, University of Science and Technology of China, Anhui, China, in 2013.

His research interests include intelligent robotics, locomotory dynamics, and the applications of shape memory alloy.



**Jiming Liu** (F'11) received the M.Eng. and Ph.D. degrees from McGill University, Montreal, QC, Canada, in 1990 and 1994, respectively.

He is the Chair Professor in computer science and the Acting Dean of the Faculty of Science at Hong Kong Baptist University, Hong Kong. His current research interests include data analytics, complex systems modeling, and collective intelligence.

Prof. Liu was the Founding Editor-in-Chief of the *Web Intelligence Journal* (IOS), an Associate Editor for Big Data and Information Analytics (AIMS), the IEEE TRANSACTIONS ON KNOWLEDGE AND DATA ENGINEERING, the IEEE TRANSACTIONS ON CYBERNETICS, and *Computational Intelligence* (Wiley), among other international journals.



**Jie Yang** received the Graduate degree from the Department of Physical Chemistry, Beijing University of Science and Technology, Beijing, China, in 1969.

He is currently a Professor in the Department of Precision Machinery and Precision Instrumentation, University of Science and Technology of China, Anhui, China. He leads several research groups focusing on intelligent robots supported by the NSF of China and 863 Project. His research interests include intelligent robots,

precision machinery materials, and high-speed photography.